Modern Pathology (2020) 33:391–403
https://doi.org/10.1038/s41379-019-0357-y

ARTICLE

AKT1 internal tandem duplications and point mutations are the genetic hallmarks of sclerosing pneumocytoma

Yi-Chen Yeh[1,2,3] · Hsiang-Ling Ho[1,4] · Yu-Chung Wu[3,5] · Chin-Chen Pan[1,3] · Yu-Chao Wang[2,6] · Teh-Ying Chou[1,7]

Received: 22 June 2019 / Revised: 5 August 2019 / Accepted: 6 August 2019 / Published online: 16 September 2019

Abstract

Sclerosing pneumocytoma is a unique benign neoplasm of the lungs. The molecular alterations in sclerosing pneumocytoma are not well understood. In a previous whole-exome sequencing study, recurrent *AKT1* point mutation was observed in about half of the cases of sclerosing pneumocytoma. However, in the remaining half, cancer-related mutations have still not been identified. In this study, we first analyzed the raw sequence data from the previous whole-exome sequencing study (PRJNA297066 cohort). Using Genomon-ITDetector, a special software for detection of internal tandem duplications, we identified recurrent internal tandem duplications in the *AKT1* gene in 22 of the 44 tumor samples (50%). All the cases positive for *AKT1* internal tandem duplications lacked *AKT1* point mutations. Next, we performed targeted next-generation sequencing in an independent cohort of sclerosing pneumocytoma from our hospital (VGH-TPE cohort), and again identified recurrent *AKT1* internal tandem duplications in 20 of the 40 (50%) tumor samples analyzed. The internal tandem duplications resulted in duplications of 7 to 16 amino acids in a narrow region of the Pleckstrin homology domain of the *AKT1* protein. This region contains the interaction interface between the Pleckstrin homology and kinase domains, which is known to play a critical role in the activation of the *AKT1* protein. Moreover, we found that *AKT1* internal tandem duplications were mutually exclusive of other forms of *AKT1* mutations, including point mutations and short indels. Taking all forms of *AKT1* mutations together, we detected *AKT1* mutations in almost all the sclerosing pneumocytomas in our study (PRJNA297066 cohort: 41 out of 44 cases, 93%; VGH-TPE cohort: 40 out of 40 cases, 100%). Our results suggest that *AKT1* mutation is the genetic hallmark of sclerosing pneumocytoma. These results would help in better understanding of the pathogenesis of sclerosing pneumocytoma.

Introduction

Sclerosing pneumocytoma is an uncommon, but unique, neoplasm of the lungs. It occurs more frequently in middle-aged adults, and is predominant in females [1]. Although sclerosing pneumocytoma is generally considered a benign neoplasm, rare cases with regional lymph node metastases and local recurrence have been reported [2–4]. Diagnosis of sclerosing pneumocytoma can be challenging, especially on fine-needle aspiration and intraoperative frozen sections, and it is frequently misdiagnosed as lung adenocarcinoma [5, 6].

Supplementary information The online version of this article (https://doi.org/10.1038/s41379-019-0357-y) contains supplementary material, which is available to authorized users.

✉ Yu-Chao Wang
yuchao@ym.edu.tw

✉ Teh-Ying Chou
tychou@vghtpe.gov.tw

[1] Department of Pathology and Laboratory Medicine, Taipei Veterans General Hospital, Taipei, Taiwan

[2] Institute of Biomedical Informatics, National Yang-Ming University, Taipei, Taiwan

[3] School of Medicine, National Yang-Ming University, Taipei, Taiwan

[4] Department of Biotechnology and Laboratory Science in Medicine, National Yang-Ming University, Taipei, Taiwan

[5] Division of Thoracic Surgery, Department of Surgery, Taipei Veterans General Hospital, Taipei, Taiwan

[6] Preventive Medicine Research Center, National Yang-Ming University, Taipei, Taiwan

[7] Institute of Clinical Medicine, National Yang-Ming University, Taipei, Taiwan

Sclerosing pneumocytoma has characteristic histopathological features. It usually displays a mixed solid, papillary, hemorrhagic, and/or sclerotic pattern, and contains two distinct cellular components, namely the round cells and the surface cells. Studies using laser microdissection and clonal analysis demonstrated that the round cells and the surface cells exhibit a uniform pattern of monoclonality, indicating that both the cell types likely originate from a common precursor [7, 8].

The histogenesis and pathogenesis of sclerosing pneumocytoma remain largely unknown at present. The molecular alterations in sclerosing pneumocytoma have been investigated in many studies. It has been shown that sclerosing pneumocytoma frequently harbors nonspecific microsatellite alterations in p16 and Rb tumor suppressor genes, but lacks alterations involving *EGFR*, *HER-2*, and *K-RAS* [9]. Besides, nuclear expression of *β-catenin* proteins is frequently seen in sclerosing pneumocytoma, indicating that Wnt/*β-catenin* pathway is involved in the pathogenesis. However, mutation in the exon 3 of *β-catenin* gene is rarely found in this tumor [10].

Recently, Jung et al. conducted a large-scale study using whole-exome sequencing to investigate genomic alterations in sclerosing pneumocytoma. They identified a high frequency of *AKT1* point mutations (overall 31 of 68, 46%) and recurrent *β-catenin* mutations (overall 3 of 68, 4%) [11]. This provides a milestone in understanding the molecular pathogenesis of sclerosing pneumocytoma. However, around half of the cases lacked identifiable cancer-related mutations in their study. This result has been particularly intriguing to us. Because sclerosing pneumocytoma is a disease with distinct and relatively uniform histopathological features, we expected that there should be a common genetic alteration in the majority of cases. We, therefore, speculated that sclerosing pneumocytoma might harbor certain kinds of genetic changes, which are difficult to detect by standard whole-exome sequencing analysis, such as structural variations, large insertions/deletions, and alterations in repetitive DNA sequences or non-coding genomic regions [12]. Internal tandem duplication, which may involve duplication of several tens to several hundreds of nucleotides within the coding exons, is also a probable genetic alteration. Internal tandem duplication is notoriously difficult to detect by standard bioinformatics pipelines, and specialized bioinformatics tools are usually required to identify this unique genetic change [13–15].

In the present study, we investigated the molecular alterations in sclerosing pneumocytoma, with a primary focus on internal tandem duplication. Using Genomon-ITDetector, a software package designed specifically for internal tandem duplication detection from cancer genome sequencing data [15], we discovered recurrent internal tandem duplications in *AKT1* gene in half of the cases. Moreover, we found that *AKT1* internal tandem duplications were mutually exclusive of other forms of *AKT1* mutations, including point mutations and short indels. Taking all forms of *AKT1* mutations together, we were able to detect *AKT1* mutations in nearly all the sclerosing pneumocytoma cases in our study. These results suggest that *AKT1* mutations are the major molecular alterations in sclerosing pneumocytoma.

Materials and methods

Analysis of PRJNA297066 sclerosing pneumocytoma cohort data

First, we analyzed the publicly available next-generation sequencing dataset for sclerosing pneumocytoma using bioinformatics tools for detecting internal tandem duplication to discover potentially unidentified molecular changes. Briefly, the raw sequence data from a total of 44 paired normal and sclerosing pneumocytoma tumor samples in the previous whole-exome sequencing study by Jung et al. (Project ID: PRJNA297066) [11] were download from the Sequence Read Archive database (https://www.ncbi.nlm.nih.gov/sra). The downloaded SRA files were converted to fastq files by *fastq-dump* in the NCBI SRA Toolkit. The sequencing reads were then aligned to the human reference genome (UCSC hg19) by Burrows–Wheeler Alignment tool to generate the aligned BAM files [16]. Genomon-ITDetector, a software package for detection of internal tandem duplications in cancer genome sequencing data, was then used to detect internal tandem duplications in the aligned BAM files [15]. Manual reviews and confirmation of the internal tandem duplications were done with Integrative Genomics Viewer [17]. The data of *AKT1* and *β-catenin* point mutations were retrieved from the manuscript by Jung et al. [11].

VGH-TPE sclerosing pneumocytoma cohort samples

We also included an independent cohort of patients with sclerosing pneumocytoma who underwent surgical resection in Taipei Veterans General Hospital between 2007 and 2017 (VGH-TPE cohort). The samples from this cohort consisted of 40 sclerosing pneumocytoma tumor samples, 25 of which had paired normal lung samples. All the tissues had been fixed in formalin before being embedded in paraffin blocks. The hematoxylin and eosin-stained slides were reviewed by a pathologist (Y.C.Y). The percentages of histological growth patterns, including hemorrhagic, solid, papillary, and sclerotic, were semi-quantitatively recorded with 5% increments for each tumor. The predominant histological pattern was then defined as the pattern with the highest percentage.

Targeted next-generation sequencing in VGH-TPE sclerosing pneumocytoma cohort

We performed targeted next-generation sequencing to sequence all exons of *AKT1* and *β-catenin* genes in the tumor and paired normal samples in the VGH-TPE sclerosing pneumocytoma cohort. Briefly, sections cut from formalin-fixed paraffin-embedded specimens were used for DNA extraction. The collected DNA was purified with GeneRead DNA FFPE Kit (Qiagen, Inc.), according to the manufacturer's instructions. The quality and quantity of the DNA were verified using NanoDrop 2000 (Thermo Fisher Scientific, Inc.) and Fragment Analyzer (Agilent formerly Advanced Analytical (AATI), Inc.). A customized DNA panel was designed using the online tool, QIAseq Targeted DNA Custom Panel Builder, covering all coding regions of *AKT1* and *β-catenin* genes. Genomic DNA samples (100 ng) were used for library preparation with multiplex PCR target enrichment panel, according to the manufacturer's instructions. The purified libraries were pooled and then sequenced with MiSeq instrument (Illumina, Inc.).

For single nucleotide variations and short indels, variant detection was performed by smCounter2 workflow, a software package for detecting somatic variants in QIAseq Targeted DNA Panel [18]. Variant allele frequency was obtained from the variant unique molecular identifier allele fraction data in the reports generated by the smCounter2. Low-frequency variants (with variant allele frequency <5%) were filtered out because they are likely to represent subclonal mutations. Synonymous mutations were also filtered out.

For detection of internal tandem duplications, the process was similar to that used for PRJNA297066 sclerosing pneumocytoma cohort data. The reads were aligned with the hg19 human reference genome using the Burrows–Wheeler Alignment tool. Detection of internal tandem duplications was performed by Genomon-ITDetector. Manual reviews of the detected internal tandem duplications were conducted using the Integrative Genomics Viewer.

Targeted PCR, gel electrophoresis, and Sanger sequencing

Hematoxylin–eosin stained tissue slides were reviewed by the pathologist to select the tumor regions. The selected tumor region was dissected manually from the corresponding areas in consecutive tissue sections and, after deparaffinization, subjected to genomic DNA extraction. Briefly, the dissected tumor tissue was transferred to an eppendorf tube containing proteinase K solution. The tube was then incubated at 56 °C for 16 h, followed by an inactivation step at 95 °C for 10 min. Exons 3 and 4 of the *AKT1* gene (NCBI reference sequence: NM_001014431.1) were amplified by PCR in a total volume of 25 μL containing 100 ng of template DNA, 1 X Taq Master Mix Red (Ampliqon III), and 0.5 μM of sense and antisense primers. The primer sequences are listed in Supplementary Table 1. The sense and antisense primers used for amplification of *AKT1* exon 3 were *AKT1*-E3S1 and *AKT1*-E3A1, and those for exon 4 were AKT-E4S1 and *AKT1*-E4A1, respectively. The PCR was carried out for 35 cycles of 95 °C for 40 s, 56 °C for 40 s, and 72 °C for 40 s, followed by 5 min extension at 72 °C. The amplicons were electrophoresed on 4% agarose gels. For *AKT1* exon 3 E17K mutation analysis, the PCR products were subjected to Sanger sequencing with *AKT1*-E3A2 primers. For *AKT1* exon 4 internal tandem duplication analysis, the PCR products, with two major bands identified on agarose gels, were extracted, purified, and then subjected to TA-cloning using T&A™ Cloning Vector Kit (Yeastern Biotech Co. Ltd., Taiwan), according to manufacturer's instructions. After transformation, single colonies were picked and subjected to Sanger sequencing with M13 forward primers.

Statistical analysis

The association of clinical and pathological characteristics with molecular alterations was analyzed by Student's *t*-test (for continuous variables), or chi-square test/Fisher's exact test (for categorical variables), when appropriate. Analyses were performed using SPSS software (IBM, Armonk, NY, USA). A *P*-value <0.05 was considered to be statistically significant.

Results

Discovery of *AKT1*-internal tandem duplication in PRJNA297066 sclerosing pneumocytoma cohort

We analyzed the whole-exome sequencing raw sequence data from PRJNA297066 sclerosing pneumocytoma cohort using the Genomon-ITDetector software, and then performed manual review with Integrative Genomics Viewer. Surprisingly, a high frequency of recurrent in-frame internal tandem duplications in the *AKT1* gene was discovered in 22 of the 44 tumor samples (50%) (Table 1, Fig. 1 and Supplementary Fig. 1). The internal tandem duplications were clustered in exon 4 of *AKT1*, which encodes the Pleckstrin homology domain of the *AKT1* protein. The internal tandem duplications were predicted to result in duplications of 7 to 15 amino acids in this region (Fig. 2a). In a subset of the cases (SH54T, SH67T, SH57T, SH41T, SH58T, SH09T, and SH03T), a novel junctional amino acid was introduced by the internal tandem duplications. In

Table 1 *AKT1* internal tandem duplication and other mutations in *AKT1* and *β-catenin* genes in the PRJNA297066 sclerosing pneumocytoma cohort

Sample ID	Patient's sex	*AKT1* internal tandem duplication	Other mutations in *AKT1* and *β-catenin* genes
SH01T	Female		*AKT1* p.E17K
SH02T	Male	p.R67_Q79dup	
SH03T	Female	p.V83_I84insSCLQWSTV	
SH04T	Female		*AKT1* p.N53H, p.E49K
SH05T	Female	p.K64_L78dup	
SH06T-1	Female		*AKT1* p.F55Y, p.L52R
SH06T-2	Female		*AKT1* p.E17K
SH07T	Female	p.M63_R76dup	
SH08T	Female	p.R67_Q79dup	
SH09T	Female	p.R76_C77insW+p.P70_R76dup	
SH10T	Female	p.P68_Q79dup	
SH11T	Female	p.T65_C77dup	
SH18T	Female		*β-catenin* p.S37F
SH20T	Female		*AKT1* p.E17K
SH23T	Female		*AKT1* p.E17K
SH25T	Female		*AKT1* p.E17K
SH34T	Female		*AKT1* p.E17K
SH36T	Female		*AKT1* p.E17K
SH37T	Male		*AKT1* p.Q79K, p.W80R
SH40T	Female		*AKT1* p.E17K
SH41T	Female	p.Q79_W80insC+p.R67_Q79dup	
SH42T	Female		*AKT1* p.E17K, p.I19L
SH43T	Female		
SH46T	Female	p.M63_R76dup	
SH47T	Female	p.K64_L78dup	
SH48T	Female		*AKT1* p.E17K
SH49T	Female	p.R67_L78dup	
SH50T	Male		
SH51T	Female	p.R67_L78dup	
SH52T	Female		*AKT1* p.E17K
SH53T	Male	p.R67_L78dup	
SH54T	Female	p.C77_L78insP+p.E66_C77dup	
SH55T	Female		*AKT1* p.E17K
SH56T	Female		*AKT1* p.Q79K, p.W80R
SH57T	Female	p.C77_L78insQ+p.R67_C77dup	
SH58T	Female	p.R76_C77insW+p.P68_R76dup	
SH59T	Female	p.R67_C77dup	
SH60T	Female		*AKT1* p.Q79K, p.W80R
SH61T	Female		*AKT1* p.Q79K, p.W80G
SH62T	Female		*AKT1* p.Q79K, p.W80R
SH63T	Female	p.R67_Q79dup	
SH64T	Female	p.R67_L78dup	
SH66T	Female	p.T65_C77dup	*β-catenin* p.S37F
SH67T	Female	p.R76_C77insS+p.E66_R76dup	

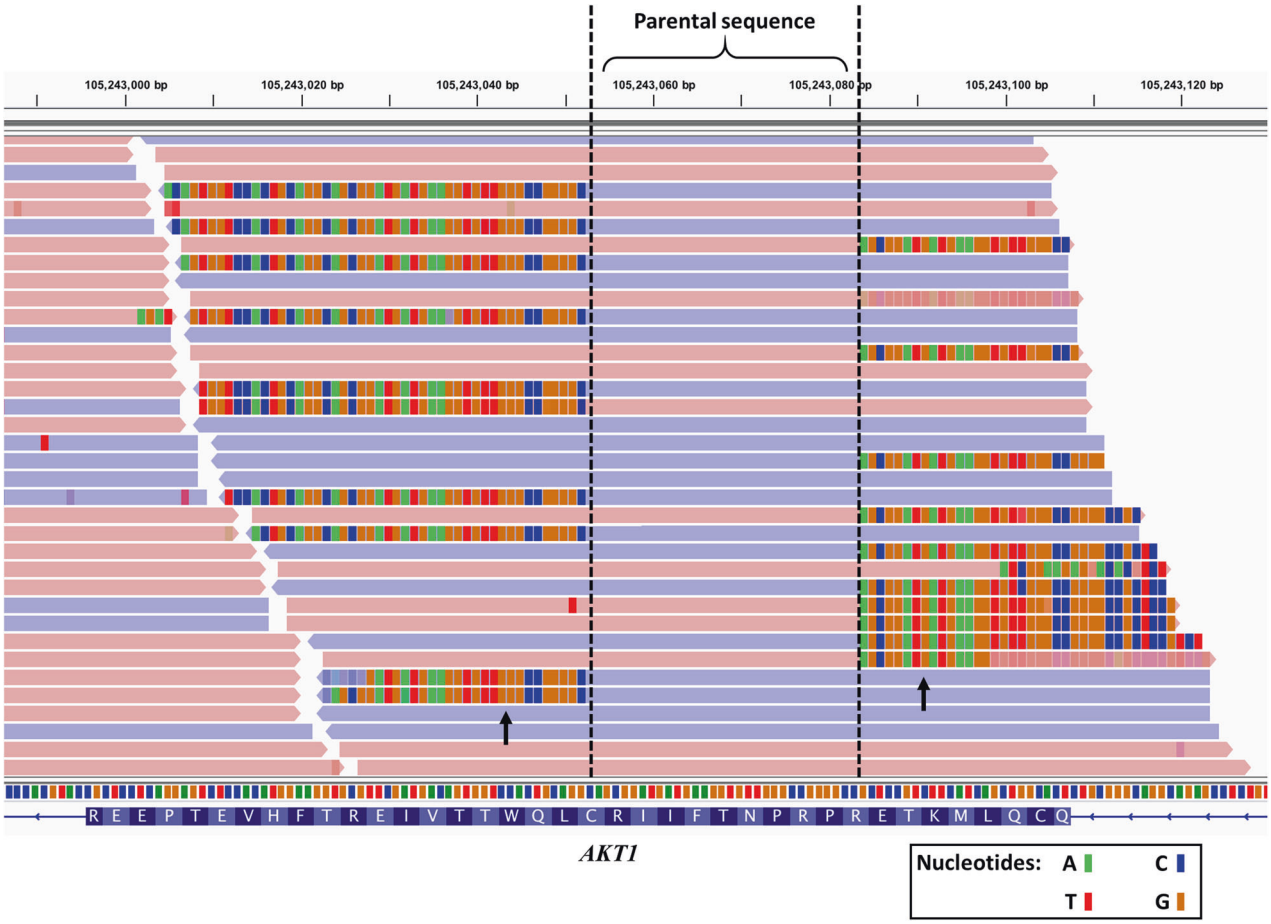

Fig. 1 Representative screenshot showing alignments around the *AKT1* exon 4 in a tumor sample (SH58T) positive for *AKT1* internal tandem duplication, using the Integrative Genomics Viewer. The regions between the two dotted lines are the parental sequences of duplicated nucleotides. The duplicated nucleotides (arrow) are aligned either to the right or left of the parental sequences, and they are marked as soft-clipped sequences by the alignment software. This is a characteristic feature of internal tandem duplications

SH03T, there was an additional point mutation in the middle of the duplicated segment, which resulted in a threonine (T) to serine (S) substitution. The *AKT1*-internal tandem duplications were only detected in the tumor samples, and were absent in all the normal samples. Moreover, we found that *AKT1*-internal tandem duplications and *AKT1* point mutations were mutually exclusive, and were found in 41 of the 44 tumor samples (93%).

Validation of *AKT1*-internal tandem duplications in the VGH-TPE sclerosing pneumocytoma cohort

To validate our findings in the PRJNA297066 sclerosing pneumocytoma cohort, we performed targeted next-generation sequencing to sequence all the exons of *AKT1* and *β-catenin* genes in an independent cohort (VGH-TPE cohort). This cohort consisted of 40 patients with sclerosing pneumocytoma who underwent surgery in our hospital. Similar to the findings in the PRJNA297066 cohort, we detected recurrent in-frame internal tandem duplications in the *AKT1* gene in 20 of the 40 tumor samples in the VGH-TPE cohort (50%) (Table 2 and Supplementary Fig. 2). The internal tandem duplications clustered in exactly the same region of the *AKT1* protein Pleckstrin homology domain as in the PRJNA297066 cohort and were predicted to result in duplications of 7 to 16 amino acids in this region (Fig. 2b). In a subset of the cases (V18T, V20T, V28T, V16T, V35T, V37T, V33T, and V04T), a novel junctional amino acid was introduced by the internal tandem duplications, which was also very similar to that observed in the PRJNA297066 cohort. In addition, in the case V23T, there was a point mutation in the middle of the duplicated segment, which resulted in a proline (P) to alanine (A) substitution. This finding was similar to that obtained for the case SH03T in the PRJNA297066 cohort.

The analysis of *AKT1* exon 4 using genomic PCR and electrophoresis on a 4% agarose gel revealed that cases carrying *AKT1*-internal tandem duplication yielded a higher molecular weight product (Fig. 3a). Sanger

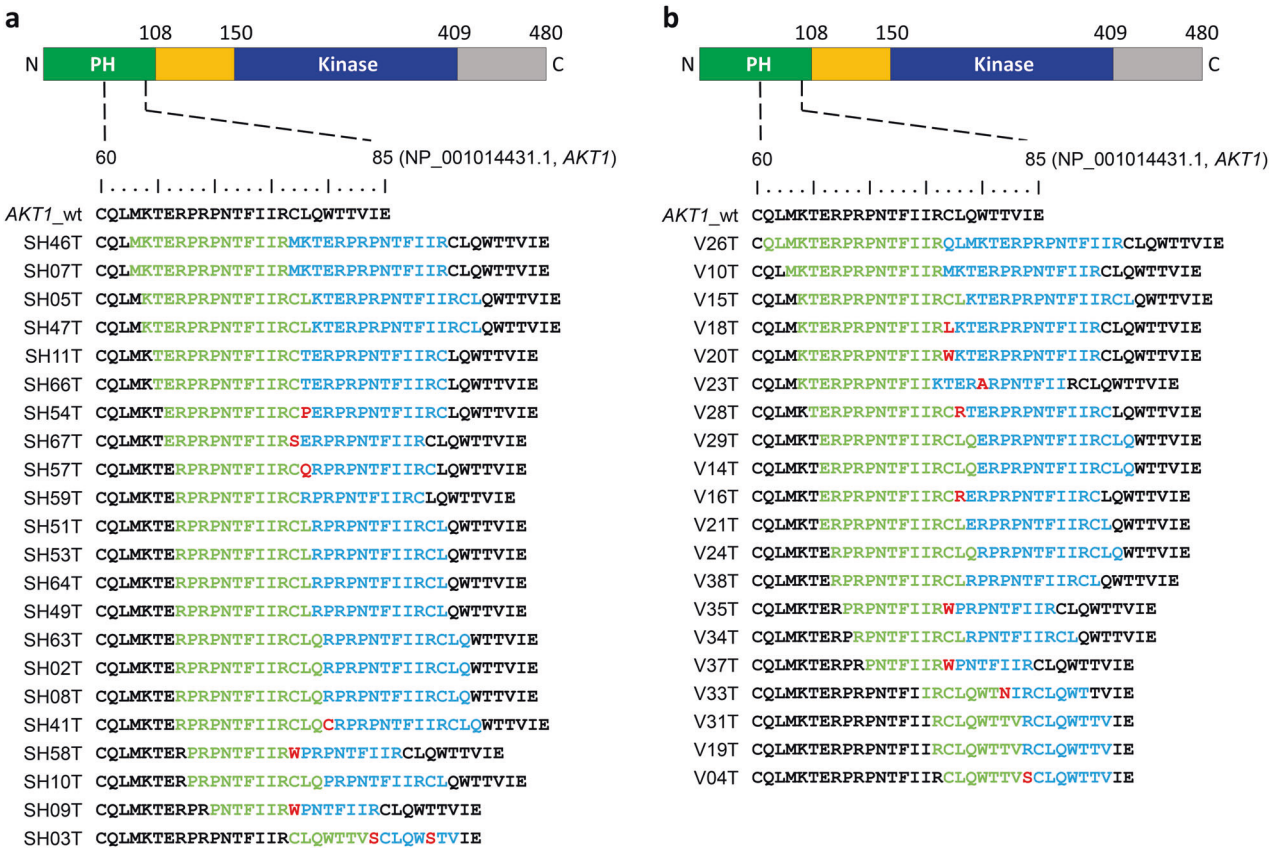

Fig. 2 **a** Schematic of the *AKT1* protein structure and predicted *AKT1* protein sequences from the tumor samples positive for internal tandem duplication in the PRJNA297066 cohort. The wild-type *AKT1* protein sequence (amino acids 60–85) is shown on the top, with the predicted protein sequence of each internal tandem duplication-positive case shown below. The first segments of the duplicated sequences are shown in green, and the second segments are shown in blue. Novel junctional amino acids (red) were introduced by the internal tandem duplications in cases SH54T, SH67T, SH57T, SH41T, SH58T, SH09T, and SH03T. In SH03T, there was an additional point mutation in the middle of the duplicated segment, which resulted in a threonine (T) to serine (S) substitution. **b** Schematic of the *AKT1* protein structure and predicted *AKT1* protein sequences from the tumor samples positive for internal tandem duplications in the VGH-TPE cohort. The wild-type *AKT1* protein sequence (amino acids 60–85) is shown on the top, with the predicted protein sequence of each internal tandem duplication-positive case shown below. The first segments of the duplicated sequences are shown in green, and the second segments are shown in blue. Novel junctional amino acids (red) were introduced by the internal tandem duplications in cases V18T, V20T, V28T, V16T, V35T, V37T, V33T, and V04T. In V23T, there was an additional point mutation in the middle of the duplicated segment, which resulted in a proline (P) to alanine (A) substitution. PH Pleckstrin homology domain, Kinase Kinase domain N N-terminal, C C-terminal

sequencing of the distinct PCR products showed the presence of in-frame tandem duplications and the duplicated sequences were identical to those derived from targeted next-generation sequencing (Fig. 3b).

In addition to *AKT1*-internal tandem duplication, we also detected other forms of *AKT1* mutations in the sclerosing pneumocytoma tumor samples (Table 2), including p.E17K (six cases) (Fig. 4), p.E17K/p.E40K (one case), p.E17K/p.I19F (one case), p.E17K/p.W80G (one case), p.E49K/p.N53H (one case), p.Q79K/p.W80G (six cases), p.Q79K/p.W80R (two cases), pW80R/p.L78_Q79insKK (one case), and p.Q79_W80delinsR/p.T81delinsMPGA (one case). Most importantly, all these *AKT1* mutations were mutually exclusive with *AKT1*-internal tandem duplications. Taking all forms of *AKT1* mutations together (including point mutations, indels, and internal tandem duplications), all sclerosing pneumocytoma tumor samples in the VGH-TPE cohort contained one of the *AKT1* mutations.

With regard to *β-catenin* genes, we detected p.S45P point mutation in one single case (V09T). However, this case also harbored the *AKT1* p.E17K mutation. The variant allele frequency of *AKT1* p.E17K mutation was 36%. In contrast, the variant allele frequency of *β-catenin* p.S45P mutation was only 9%. The low variant allele frequency of *β-catenin* p.S45P mutation suggested that this mutation was present in a subclone of tumor cells, and was likely to be a secondary event during tumor progression.

No *AKT1* or *β-catenin* mutations were detected in normal samples of the VGH-TPE cohort. The pie charts of *AKT1*

Table 2 *AKT1* internal tandem duplications and other mutations in *AKT1* and *β-catenin* genes in the VGH-TPE sclerosing pneumocytoma cohort

Sample ID	Patient's sex	Histology	*AKT1* internal tandem duplication	Other mutations in *AKT1* and *β-catenin* genes
V01T	Female	Papillary		*AKT1* p.E17K
V02T	Male	Hemorrhagic		*AKT1* p.E17K; p.E40K
V03T	Female	Hemorrhagic		*AKT1* p.Q79K; p.W80G
V04T	Female	Papillary	p.V83_I84insS+p.C77_V83dup	
V05T	Female	Solid		*AKT1* p.E17K
V06T	Female	Solid		*AKT1* p.E17K; p.W80G
V07T	Female	Hemorrhagic		*AKT1* p.E17K
V08T	Female	Papillary		*AKT1* p.E17K; p.I19F
V09T	Female	Hemorrhagic		*AKT1* p.E17K; *β-catenin* p.S45P
V10T	Female	Hemorrhagic	p.M63_R76dup	
V11T	Male	Papillary		*AKT1* p.Q79K; p.W80G
V12T	Female	Solid		*AKT1* p.Q79K; p.W80R
V13T	Female	Solid		*AKT1* p.Q79K; p.W80G
V14T	Female	Hemorrhagic	p.E66_Q79dup	
V15T	Female	Hemorrhagic	p.K64_L78dup	
V16T	Female	Hemorrhagic	p.C77_L78insR+p.E66_C77dup	
V17T	Female	Solid		*AKT1* p.E17K
V18T	Female	Sclerotic	p.R76_C77insL+p.K64_R76dup	
V19T	Female	Hemorrhagic	p.R76_V83dup	
V20T	Female	Papillary	p.R76_C77insW+p.K64_R76dup	
V21T	Female	Solid	p.E66_L78dup	
V22T	Male	Papillary		*AKT1* p.Q79K; p.W80R
V23T	Female	Papillary	p.I75_R76insKTERARPNTFII	
V24T	Female	Papillary	p.R67_Q79dup	
V25T	Male	Papillary		*AKT1* p.Q79K; p.W80G
V26T	Female	Papillary	p.Q61_R76dup	
V27T	Female	Solid		*AKT1* p.E49K; p.N53H
V28T	Female	Papillary	p.C77_L78insR+p.T65_C77dup	
V29T	Female	Solid	p.E66_Q79dup	
V30T	Female	Solid		*AKT1* p.E17K
V31T	Female	Solid	p.R76_V83dup	
V32T	Female	Sclerotic		*AKT1* p.W80R; p.L78_Q79insKK
V33T	Female	Solid	pT81_T82insN+p.I75_T81dup	
V34T	Female	Solid	p.R69_L78dup	
V35T	Female	Solid	p.R76_C77_insW+p.P68_R76dup	
V36T	Female	Papillary		*AKT1* p.Q79K; p.W80G
V37T	Female	Hemorrhagic	p.R76_C77insW+p.P70_R76dup	
V38T	Female	Papillary	p.R67_L78dup	
V39T	Female	Hemorrhagic		*AKT1* p.Q79_W80delinsR; p.T81delinsMPGA
V40T	Female	Hemorrhagic		*AKT1* p.Q79K; p.W80G

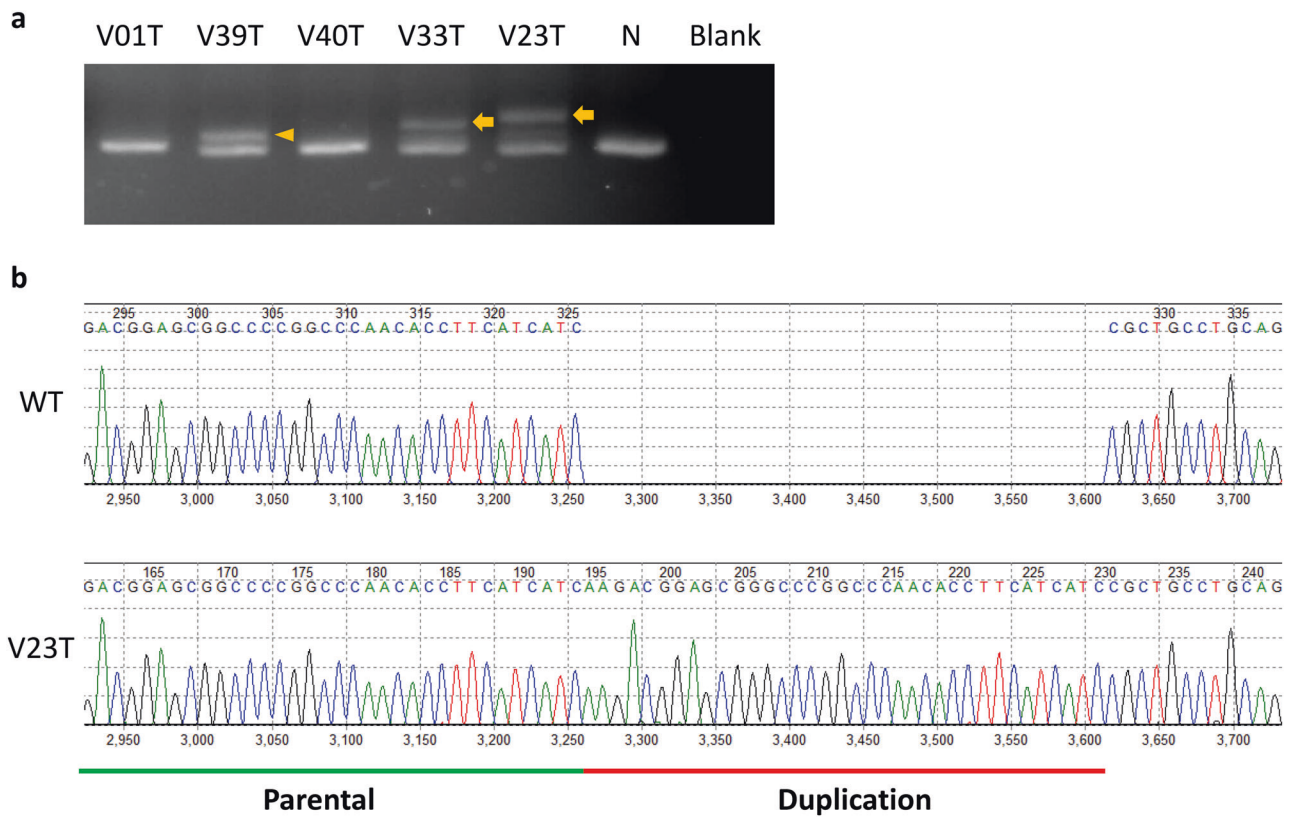

Fig. 3 **a** Targeted PCR and gel electrophoresis of *AKT1* exon 4 from five representative samples (V01T, V39T, V40T, V33T, and V23T) in the VGH-TPE cohort. In samples positive for *AKT1*, internal tandem duplication (V33T and V23T), large PCR products corresponding to the internal tandem duplications were detected (arrow), in addition to the expected wild-type products. In samples V01T and V40T, which are negative for *AKT1* internal tandem duplication, only wild-type products were detected. In sample V39T, an additional PCR product, slightly larger than the wild-type product, was also detected (arrowhead), which corresponds to the complex *AKT1* mutation of p.Q79_W80delinsR and p.T81delinsMPGA in this case. **b** Sanger sequencing from a representative sample (V23T) positive for *AKT1* internal tandem duplication showed the duplicated sequence. N normal lung, WT wild type

and *β-catenin* mutations in the PRJNA297066 cohort and VGH-TPE cohort are shown in Fig. 5.

Correlation between clinicopathological characteristics and *AKT1* mutations in the VGH-TPE sclerosing pneumocytoma cohort

We analyzed the correlation between clinicopathological characteristics and *AKT1* mutations in the VGH-TPE cohort, and the results are summarized in Table 3. There were no significant differences in clinical characteristics or pathological features between patients with *AKT1*-internal tandem duplication or other types of *AKT1* mutations (Fig. 6). We noticed that all the male patients in the VGH-TPE cohort belonged to the group with other types of *AKT1* mutations. However, this was probably due to chance because we observed that two male patients in the PRJNA297066 cohort belonged to the group with *AKT1*-internal tandem duplication (SH53T and SH02T).

Discussion

In this study, we demonstrate that *AKT1* mutation is present in nearly all the sclerosing pneumocytomas, with internal tandem duplication and point mutations being the most common forms. *AKT1* belongs to the AKT kinase family, the members of which serve as critical downstream effectors of phosphatidylinositol-3 kinase (PI3K) signaling. Under basal conditions, *AKT1* localizes to the cytosol, and maintains an inactive closed "PH-in" conformation through the interaction between its Pleckstrin homology and kinase domains [19]. Following activation of phosphatidylinositol-3 kinase by proliferative signals, the inactive *AKT1* in the cytosol is recruited to the plasma membrane through binding of the Pleckstrin homology domain. This results in a conformational change that separates the Pleckstrin homology and kinase domains, shifting *AKT1* to an open "PH-out" state. The PH-out state enables phosphorylation of Thr308 and Ser473

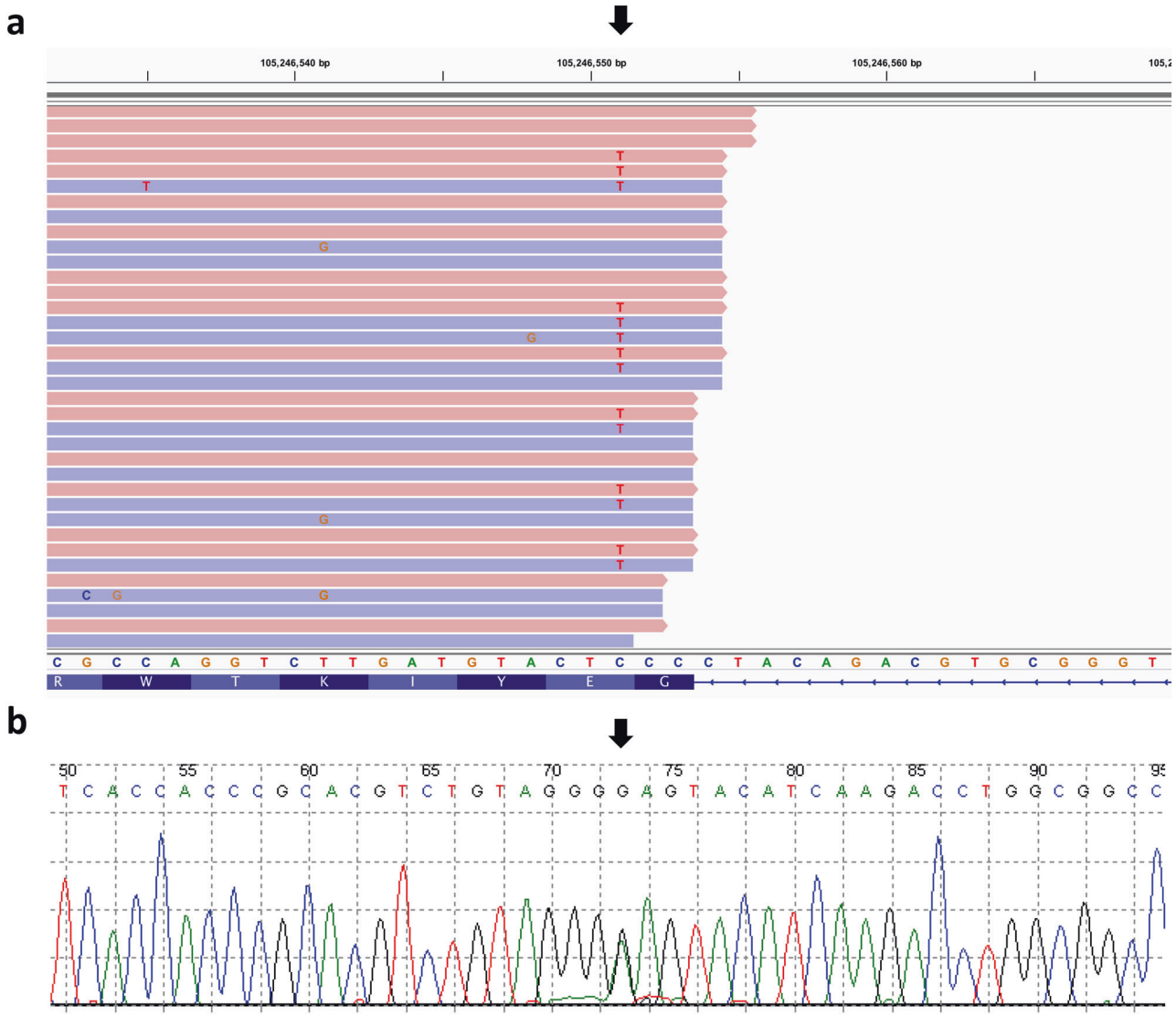

Fig. 4 **a** Screenshot for a representative sample (V01T) showing *AKT1* p.E17K (c.49G>A) mutation, using Integrative Genomics Viewer. The reference sequence shown in Integrative Genomics Viewer is the antisense strand of *AKT1*, and the corresponding nucleotide change for p.E17K mutation is C>T mutation (arrow). **b** Sanger sequencing from the same sample confirmed the *AKT1* p.E17K (c.49G>A) mutation (arrow)

residues of *AKT1*, which leads to maximal activation of the kinase [20].

The PI3K–AKT pathway is one of the most commonly dysregulated pathways in cancer. Gain-of-function mutations in *AKT1* have been identified in a broad range of tumor types, with *AKT1* p.E17K being the most frequent hotspot [21]. The pathogenic role of *AKT1* p.E17K mutation has been well studied. Structural studies have shown that *AKT1* p.E17K mutation directly alters the electrostatic interactions of the lipid-binding pocket of the Pleckstrin homology domain and activates *AKT1* through pathological localization to the plasma membrane. This mechanism stimulates downstream signaling and leads to oncogenic transformation [22].

In contrast, little is known regarding the role of *AKT1* internal tandem duplications in oncogenesis. In the literature, there are very few reports of *AKT1* internal tandem duplications in human cancers. To the best of our knowledge, only juvenile granulosa cell tumor and breast cancer have been reported to harbor *AKT1* internal tandem duplications [23, 24]. The affected genomic region in juvenile granulosa cell tumor and breast cancer is exactly the same as observed in sclerosing pneumocytoma. In juvenile granulosa cell tumor, the *AKT1* internal tandem duplication was detected in 10 out of 16 case (63%). In addition, there was also a high frequency of recurrent *AKT1* point mutations (10 out of 16 cases, 63%) [23]. However, unlike in sclerosing pneumocytoma, the *AKT1* internal tandem duplication and point

Table 3 Characteristics of patients with *AKT1*-internal tandem duplications or other forms of *AKT1* mutations in the VGH-TPE cohort

	AKT1-internal tandem duplication ($n = 20$)	Other *AKT1* mutations ($n = 20$)	Total ($n = 40$)	*P*-value
Age (year, mean ± standard deviation)	52.7 ± 13.8	47.7 ± 13.5	50.2 ± 13.7	0.258[a]
Sex				
Female	20 (100%)	16 (80%)	36 (90%)	0.106[b]
Male	0 (0%)	4 (20%)	4 (10%)	
Location				0.113[b]
Right lung	13 (65%)	8 (40%)	21 (53%)	
Left lung	7 (35%)	12 (60%)	19 (48%)	
Tumor size (cm, mean ± standard deviation)	2.0 ± 1.2	2.3 ± 1.3	2.2 ± 1.2	0.460[a]
Histology pattern				0.985[b]
Hemorrhagic	6 (30%)	6 (30%)	12 (30%)	
Papillary	7 (35%)	6 (30%)	13 (33%)	
Sclerotic	1 (5%)	1 (5%)	2 (5%)	
Solid	6 (30%)	7 (35%)	13 (33%)	

[a]Student's *t*-test

[b]Chi-squared test or Fisher's exact test

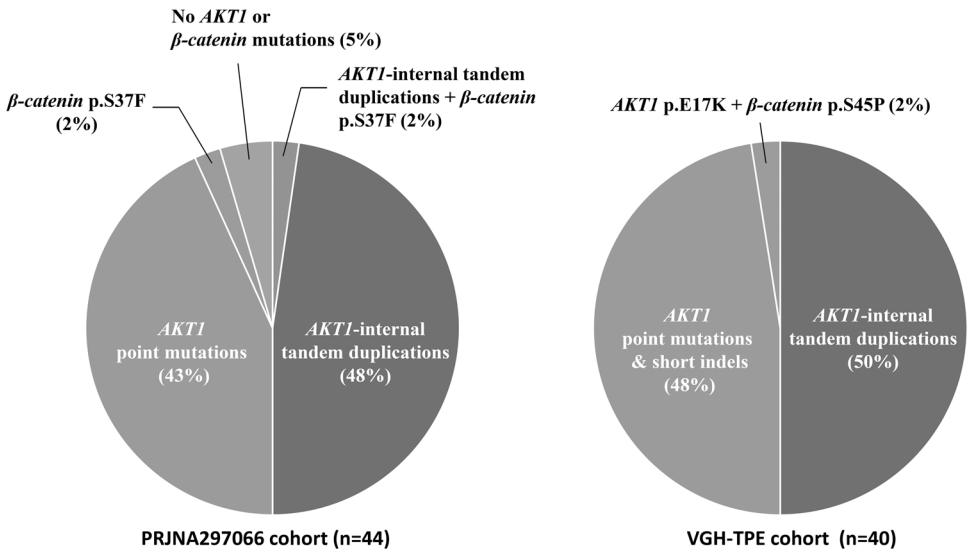

Fig. 5 Pie charts of *AKT1* and *β-catenin* mutations in the PRJNA297066 and VGH-TPE cohorts

mutations in juvenile granulosa cell tumor do not appear to be mutually exclusive. Another interesting finding is that the sites of *AKT1* point mutations in sclerosing pneumocytoma are restricted to the Pleckstrin homology domain, whereas in juvenile granulosa cell tumor, many *AKT1* point mutations occur outside the Pleckstrin homology domain. In breast cancer, the existence of *AKT1* internal tandem duplication was identified very recently in a large-scale study by Chang et al. [24]. In this study, *AKT1* point mutations (p.E17K) were detected in 80 out of 2561 cases (3%), whereas *AKT1* internal tandem duplications were only detected in 2 out of 2559 cases (0.08%), which is very intriguing. In sclerosing pneumocytoma and juvenile granulosa cell tumor, the frequencies of *AKT1* internal tandem duplications and point mutations were nearly equal. However, there appears to be a substantial difference between the frequency of *AKT1* point mutations and *AKT1* internal tandem duplications in breast cancer.

The pathogenic mechanisms of *AKT1* internal tandem duplications are not well understood. It is noticeable that the insertion points of duplicated sequences in *AKT1* internal tandem duplications clustered at amino acids 76–85 of *AKT1* protein, which contains the region of

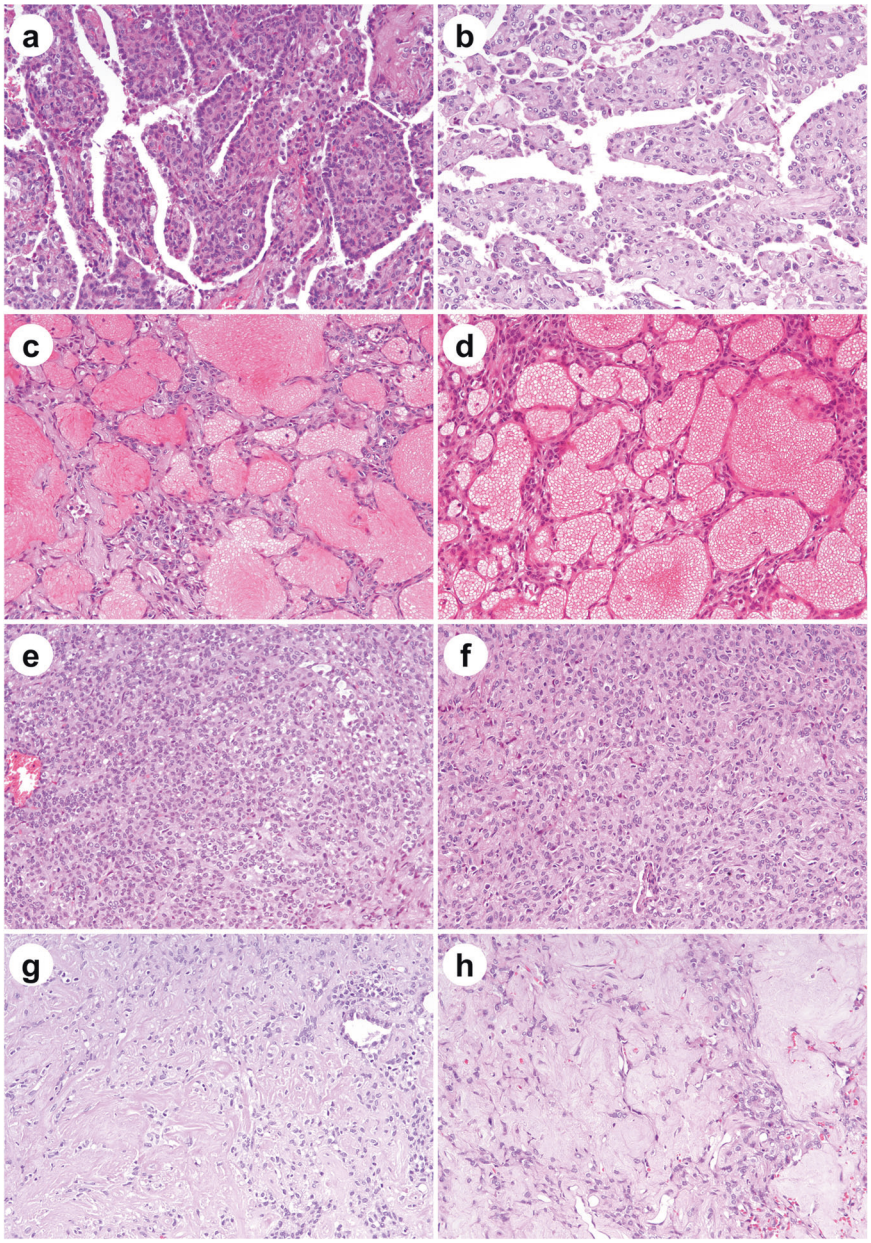

Fig. 6 Representative histological features of cases with *AKT1* point mutations or short indels (**a**, **c**, **e**, **g**), and cases with *AKT1* internal tandem duplication (**b**, **d**, **f**, **h**). **a** A case (V01T) with *AKT1* p.E17K mutation showing papillary pattern. **b** A case (V26T) with *AKT1*-internal tandem duplication showing papillary pattern. **c** A case (V07T) with *AKT1* p.E17K mutation showing hemorrhagic pattern. **d** A case (V19T) with *AKT1*-internal tandem duplication showing hemorrhagic pattern. **e** A case (V12T) with *AKT1* p.Q79K; p.W80R mutation showing solid pattern. **f** A case (V35T) with *AKT1*-internal tandem duplication showing solid pattern. **g** A case (V32T) with *AKT1* p.W80R; p.L78_Q79insKK mutation showing sclerotic pattern. **h** A case (V18T) with *AKT1*-internal tandem duplication showing sclerotic pattern (original magnification:×200)

Pleckstrin homology domain and kinase domain interaction interface (Fig. 7) [19]. It has been shown that disruption of Pleckstrin homology domain and kinase domain interactions by point mutations at the Pleckstrin homology domain and kinase domain interaction interface leads to oncogenic activation of AKT in human cancers [19]. It seems plausible that the *AKT1* internal tandem duplications occurring at this region might also disturb Pleckstrin homology domain and kinase domain interactions, and lead to oncogenic activation of AKT. To verify this speculation, further structural studies are required. However, in studies on cell lines, it has been shown that HeLa cells and human mammary gland cells (MCF10A) transfected with *AKT1* internal tandem duplication mutation constructs display high level of *AKT1* phosphorylation and activation [23, 24]. Furthermore, cells transfected with *AKT1* internal tandem duplication mutation constructs demonstrated sensitivity to the AKT kinase inhibitor, AZD5363, indicating the therapeutic implications of *AKT1* internal tandem duplication [24, 25].

In conclusion, our results show that *AKT1* mutations, including internal tandem duplication, point mutations, and short indels, are present in nearly all sclerosing pneumocytomas. These mutations are mutually exclusive of each other. All these mutations occur in the Pleckstrin homology domain, a critical component in the activation

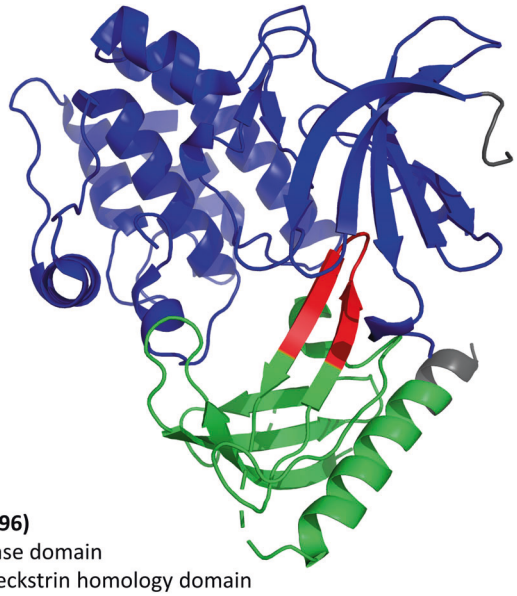

Fig. 7 Ribbon representation of Pleckstrin homology domain (green) and kinase domain (blue) of *AKT1* protein (Protein Data Bank ID code 3O96). The insertion points of duplicated sequences in *AKT1* internal tandem duplication clustered at amino acids 76–85 (red), which involve the region of the interaction interface between the Pleckstrin homology domain and kinase domain

of the *AKT1* protein. Our results suggest that *AKT1* mutation is the genetic hallmark of sclerosing pneumocytoma.

Acknowledgements The authors are grateful to Wen-Yu Hsieh and Chun-An Kuo for providing technical assistance, and to the Biobank, Taipei Veterans General Hospital for assistance with sample preparation in this study. This work was supported by Ministry of Science and Technology, Taiwan (MOST 106-2221-E-010-019-MY3, MOST 107-2320-B-075-004), and Taipei Veterans General Hospital, Taipei, Taiwan (V108B-001).

Compliance with ethical standards

Conflict of interest The authors declare that they have no conflict of interest.

Publisher's note Springer Nature remains neutral with regard to jurisdictional claims in published maps and institutional affiliations.

References

1. Devouassoux-Shisheboran M, Hayashi T, Linnoila RI, Koss MN, Travis WD. A clinicopathologic study of 100 cases of pulmonary sclerosing hemangioma with immunohistochemical studies: TTF-1 is expressed in both round and surface cells, suggesting an origin from primitive respiratory epithelium. Am J Surg Pathol. 2000;24:906–16.
2. Adachi Y, Tsuta K, Hirano R, Tanaka J, Minamino K, Shimo T, et al. Pulmonary sclerosing hemangioma with lymph node metastasis: a case report and literature review. Oncol Lett. 2014;7:997–1000.
3. Kalhor N, Staerkel GA, Moran CA. So-called sclerosing hemangioma of lung: current concept. Ann Diagn Pathol. 2010;14:60–7.
4. Wei S, Tian J, Song X, Chen Y. Recurrence of pulmonary sclerosing hemangioma. Thorac Cardiovasc Surg. 2008;56:120–2.
5. Lim JH, Lee N, Choi DW, Oh HJ, Park HY, Kim KH, et al. Pulmonary sclerosing pneumocytoma mimicking lung cancer: Case report and review of the literature. Thorac Cancer. 2016;7:508–11.
6. Yang CH, Lee LY. Pulmonary sclerosing pneumocytoma remains a diagnostic challenge using frozen sections: a clinicopathological analysis of 59 cases. Histopathology. 2018;72:500–8.
7. Niho S, Suzuki K, Yokose T, Kodama T, Nishiwaki Y, Esumi H. Monoclonality of both pale cells and cuboidal cells of sclerosing hemangioma of the lung. Am J Pathol. 1998;152:1065–9.
8. Wang EH, Dai SD, Qi FJ, Hong-Tao X, Wei Q. Gene expression and clonality analysis of the androgen receptor and phosphoglycerate kinase genes in polygonal cells and cuboidal cells in so-called pulmonary sclerosing hemangioma. Mod Pathol. 2007;20:1208–15.
9. Sartori G, Bettelli S, Schirosi L, Bigiani N, Malorana A, Cavazza A, et al. Microsatellite and EGFR, HER2 and K-RAS analyses in sclerosing hemangioma of the lung. Am J Surg Pathol. 2007;31:1512–20.
10. Chiang PM, Yuan RH, Hsu HC, Mao TL, Hu RH, Lai PL, et al. Frequent nuclear expression of beta-catenin protein but rare beta-catenin mutation in pulmonary sclerosing haemangioma. J Clin Pathol. 2008;61:268–71.
11. Jung SH, Kim MS, Lee SH, Park HC, Choi HJ, Maeng L, et al. Whole-exome sequencing identifies recurrent *AKT1* mutations in sclerosing hemangioma of lung. Proc Natl Acad Sci USA. 2016;113:10672–7.
12. Yohe S, Thyagarajan B. Review of clinical next-generation sequencing. Arch Pathol Lab Med. 2017;141:1544–57.
13. Spencer DH, Abel HJ, Lockwood CM, Payton JE, Szankasi P, Kelley TW, et al. Detection of FLT3 internal tandem duplication in targeted, short-read-length, next-generation sequencing data. J Mol Diagn. 2013;15:81–93.
14. Roy A, Kumar V, Zorman B, Fang E, Haines KM, Doddapaneni, et al. Recurrent internal tandem duplications of BCOR in clear cell sarcoma of the kidney. Nat Commun. 2015;6:8891.
15. Chiba K, Shiraishi Y, Nagata Y, Yoshida K, Imoto S, Ogawa S, et al. Genomon ITDetector: a tool for somatic internal tandem duplication detection from cancer genome sequencing data. Bioinformatics. 2015;31:116–8.
16. Li H, Durbin R. Fast and accurate short read alignment with Burrows-Wheeler transform. Bioinformatics. 2009;25:1754–60.
17. Thorvaldsdottir H, Robinson JT, Mesirov JP. Integrative Genomics Viewer (IGV): high-performance genomics data visualization and exploration. Brief Bioinform. 2013;14:178–92.
18. Xu C, Gu X, Padmanabhan R, Wu Z, Peng Q, DiCarlo J, et al. smCounter2: an accurate low-frequency variant caller for targeted sequencing data with unique molecular identifiers. Bioinformatics. 2019;35:1299–309.
19. Parikh C, Janakiraman V, Wu WI, Foo CK, Kljavin NM, Chaudhuri S, et al. Disruption of PH-kinase domain interactions leads to oncogenic activation of AKT in human cancers. Proc Natl Acad Sci USA. 2012;109:19368–73.
20. Manning BD, Toker A. AKT/PKB signaling: navigating the network. Cell. 2017;169:381–405.

21. Mundi PS, Sachdev J, McCourt C, Kalinsky K. AKT in cancer: new molecular insights and advances in drug development. Br J Clin Pharm. 2016;82:943–56.
22. Carpten JD, Faber AL, Horn C, Donoho GP, Briggs SL, Robbins CM, et al. A transforming mutation in the pleckstrin homology domain of *AKT1* in cancer. Nature. 2007;448:439–44.
23. Bessiere L, Todeschini AL, Auguste A, Sarnacki S, Flatters D, Legois B, et al. A hot-spot of in-frame duplications activates the oncoprotein *AKT1* in juvenile granulosa cell tumors. EBioMedicine. 2015;2:421–31.
24. Chang MT, Bhattarai TS, Schram AM, Bielski CM, Donoghue MTA, Jonsson P, et al. Accelerating discovery of functional mutant alleles in cancer. Cancer Discov. 2018;8:174–83.
25. Hyman DM, Smyth LM, Donoghue MTA, Westin SN, Bedard PL, Dean EJ, et al. AKT Inhibition in Solid Tumors With *AKT1* Mutations. J Clin Oncol. 2017;35:2251–9.